A Homolog of *Blade-On-Petiole 1* and *2* (*BOP1/2*) Controls Internode Length and Homeotic Changes of the Barley Inflorescence[1][OPEN]

Matthias Jost[2], Shin Taketa[2], Martin Mascher, Axel Himmelbach, Takahisa Yuo, Fahimeh Shahinnia, Twan Rutten, Arnis Druka[3], Thomas Schmutzer, Burkhard Steuernagel[4], Sebastian Beier, Stefan Taudien, Uwe Scholz, Michele Morgante, Robbie Waugh, and Nils Stein*

Leibniz Institute of Plant Genetics and Crop Plant Research, Gatersleben, 06466 Stadt Seeland, Germany (M.J., Ma.M., A.H., F.S., T.R., T.S., B.S., S.B., U.S., N.S.); Institute of Plant Science and Resources, Okayama University, Okayama 710–0046, Japan (Sh.T., T.Y.); James Hutton Institute, Invergowrie, Dundee DD2 5DA, United Kingdom (A.D., R.W.); Leibniz Institute on Aging and Fritz-Lipmann Institute, 07745 Jena, Germany (St.T.); Applied Genomics Institute, University of Udine, 33100 Udine, Italy (Mi.M.); and Division of Plant Sciences, University of Dundee, Dundee DD1 4HN, United Kingdom (R.W.)

ORCID IDs: 0000-0001-7338-0946 (A.H.); 0000-0001-8236-7647 (F.S.); 0000-0001-5891-6503 (T.R.); 0000-0003-3663-2694 (A.D.); 0000-0001-8796-1768 (M.J.); 0000-0003-1073-6719 (T.S.); 0000-0002-8284-7728 (B.S.); 0000-0001-6113-3518 (U.S.); 0000-0003-1045-3065 (R.W.); 0000-0003-3011-8731 (N.S.).

Inflorescence architecture in small-grain cereals has a direct effect on yield and is an important selection target in breeding for yield improvement. We analyzed the recessive mutation *laxatum-a* (*lax-a*) in barley (*Hordeum vulgare*), which causes pleiotropic changes in spike development, resulting in (1) extended rachis internodes conferring a more relaxed inflorescence, (2) broadened base of the lemma awns, (3) thinner grains that are largely exposed due to reduced marginal growth of the palea and lemma, and (4) and homeotic conversion of lodicules into two stamenoid structures. Map-based cloning enforced by mapping-by-sequencing of the mutant *lax-a* locus enabled the identification of a homolog of *BLADE-ON-PETIOLE1* (*BOP1*) and *BOP2* as the causal gene. Interestingly, the recently identified barley *uniculme4* gene also is a *BOP1/2* homolog and has been shown to regulate tillering and leaf sheath development. While the Arabidopsis (*Arabidopsis thaliana*) *BOP1* and *BOP2* genes act redundantly, the barley genes contribute independent effects in specifying the developmental growth of vegetative and reproductive organs, respectively. Analysis of natural genetic diversity revealed strikingly different haplotype diversity for the two paralogous barley genes, likely affected by the respective genomic environments, since no indication for an active selection process was detected.

The inflorescence is the most prominent part of small-grain cereal plants, producing the carbohydrate-rich grains that are harvested for food, feed, and fiber. However, our understanding of the genetic factors that regulate inflorescence architecture remains limited. What is clear is that the appearance and shape of the inflorescence has been under constant visual selection since early domestication and is still ongoing in modern plant breeding due to the impact of inflorescence architecture on crop yield. For instance, in barley (*Hordeum vulgare*), strong selection has been exerted on spontaneously occurring alleles of *non-brittle rachis1* (*btr1*) and *btr2* that prevent dehiscence of the rachis at maturity (Pourkheirandish et al., 2015), *six-rowed spike1* (*vrs1*) that determines whether the inflorescence exhibits two or six rows of grain (Komatsuda et al., 2007), and *nudum* (*nud*) that controls whether the grain is hulled or hull-less (Taketa et al., 2008). Ultimately, knowing all of the genes that control cereal inflorescence architecture will provide targets for understanding and exploiting natural or induced genetic diversity toward improving both yield potential and end-use characteristics.

The barley inflorescence or spike forms an unbranched main rachis carrying triplets of sessile single-floreted

spikelets, inserted at opposing sides of subsequent rachis nodes, that leads to the characteristic two-rowed (lateral spikelets infertile) or six-rowed (all three spikelets at a node are fertile) phenotype of domesticated barley. Each fertile barley floret is composed of a central carpel surrounded by a whorl of three stamens and two lodicules and enclosed by two leaf-like structures, the palea and the generally long-awned lemma (Kellogg, 2001). The genes controlling barley inflorescence architecture and development have only been revealed for a few characters. Major genes that control row type (*vrs1* [Komatsuda et al., 2007], *intermedium-c* [Ramsay et al., 2011], and *vrs4* [Koppolu et al., 2013]), the conversion of awns into an extra floret (*Hooded*; Müller et al., 1995), adherence of the hull to the caryopsis (*nud*; Taketa et al., 2008), swelling of lodicules conferring open/closed flowering (cleistogamy/chasmogamy) and spike density (*cly1* [Nair et al., 2010] and *zeo1* [Houston et al., 2013]), elongation of awns and pistil morphology (*lks2*; Yuo et al., 2012), suppression of bracts (*trd1*; Whipple et al., 2010; Houston et al., 2012), spike branching (*com2*; Poursarebani et al., 2015), and brittleness of the rachis (*btr1/btr2*; Pourkheirandish et al., 2015) were recently cloned. A large number of additional morphological mutants that influence barley inflorescence development (Forster et al., 2007) also have been described, and the underlying genes need to be identified to reach a more complete understanding of the regulatory pathways controlling barley spike architecture and development (Forster et al., 2007).

The recessive *laxatum-a* (*lax-a*) mutant exhibits a pleiotropically altered spike architecture characterized by (1) extended rachis internodes conferring a relaxed inflorescence architecture, (2) a broadened base of the lemma awns, (3) thin and exposed grains due to an impaired palea development, as well as (4) a homeotic conversion of the lodicules into two additional stamens, which are smaller and have only two locules instead of four in the regular three stamens (Larsson, 1985; Laurie et al., 1996).

Here, we describe the identification and characterization of the gene that is disrupted in the *lax-a.8* mutant. Located in a region of severely suppressed recombination frequency, the gene was identified using an innovative mapping-by-sequencing and cloning-by-sequencing approach. It encodes a homolog of the Arabidopsis (*Arabidopsis thaliana*) putative transcriptional coactivator genes *BLADE-ON-PETIOLE1* (*BOP1*) and *BOP2*. Similarities in the morphological defects of *BOP-like* mutants indicated a partially conserved function between Arabidopsis and barley.

RESULTS

The *lax-a* Phenotype

The original *lax-a.8* mutant was obtained by fast-neutron mutagenesis of cv Bonus (Franckowiak and Lundqvist, 2010). For genetic analysis, the mutation was introgressed previously by repeated backcrossing into cv Bowman to produce the nearly isogenic line (NIL) BW457 (Druka et al., 2011). The term laxatum refers to its relaxed (lax) spike phenotype, which is manifested by an average 15% increase of rachis internode length in BW457 compared with wild-type cv Bowman (Supplemental Fig. S1). The unique pleiotropic characteristics of *lax-a* set it apart from other laxatum-type mutants: its awns have a broad base, and its lodicules are homeotically converted into stamens of smaller size and comprising only two instead of four locules (Fig. 1). The thin and angular grains of *lax-a* mutants are exposed at spike maturity. This is the result of the incomplete covering of grains by the outer lemma and inner palea due to impaired development of their marginal regions. Interestingly, *lax-a* flowers can open without the impetus force of lodicule swelling (Fig. 1).

Mapping-by-Sequencing of Pooled Recombinant Plants Revealed a Candidate Gene for the *lax-a* Mutation

We performed conventional high-resolution genetic mapping followed by exome-capture sequencing of selected recombinant plants to identify a candidate gene for the *lax-a* locus. The NIL BW457 carried a 38.5-centimorgan (cM) introgression interval on chromosome 5H harboring the mutant locus (Druka et al., 2011). Initial low-resolution mapping allocated the gene to a 1.5-cM interval. The *lax-a* phenotype cosegregated with a cluster of four markers spanning the genetic centromere of chromosome 5H (Supplemental Fig. S2). Mapping was extended to a population of 1,970 F2 plants that delimited an interval of 0.2 cM on the long arm of chromosome 5H (Supplemental Fig. S2). The rather small genetic interval was related to a large physical interval and was predicted to contain a minimum of 200 genes based on the analysis of conserved synteny to sequenced model grass genomes (Mayer et al., 2011). Thus, the gene was located in a region with significantly reduced recombination frequency: a characteristic, typical in barley, for loci at close proximity to the genetic centromere (Mayer et al., 2012). All flanking markers were anchored by sequence comparison with the physical map of barley (Mayer et al., 2012), but a single physical map contig could not be identified (Table I).

We continued with a mapping-by-sequencing strategy for marker saturation, fine-mapping, and candidate gene identification by whole exome-capture resequencing of recombinant plants. Eight recombination events characterized the high-resolution genetic mapping interval of 0.2 cM carrying the gene *lax-a*. The respective eight recombinant F2 plants could be grouped into five different classes of recombinant haplotype/phenotype combinations that we called lax-1 to lax-5 (Fig. 2A). DNAs of individuals belonging to the same class were then pooled for target-enrichment shotgun resequencing (Mascher et al., 2013a). More than 30 million properly paired sequence reads were obtained
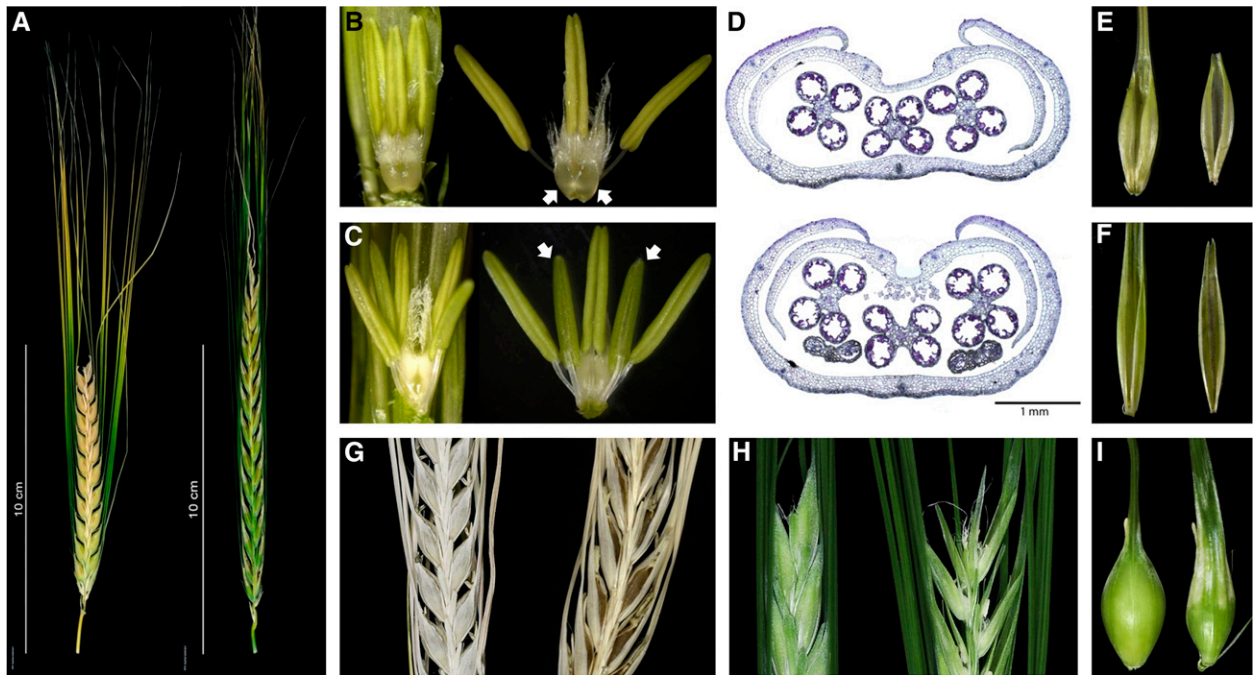
Figure 1. The *lax-a* phenotype of BW457. A, The *lax-a* phenotype is characterized by an increased spike length caused by 15% longer rachis internodes compared with the wild type (Supplemental Fig. S1). B and C, Lodicules of wild-type plants (B) are homeotically converted into additional stamenoid organs in *lax-a* mutants (C). D, Cross sections through young wild-type (top) and *lax-a* (bottom) florets showing that the additional stamens are smaller and comprise only two instead of four locules. E to H, Compared with wild-type lemma and palea (E), the *lax-a* palea and lemma are much more narrow (F), which leads to exposed and visible caryopses in mature *lax-a* inflorescences (right sample; G) and causes opening of flowers in *lax-a* mutants (right) while wild-type flowers stay closed (H). I, Awns of *lax-a* plants (right) have a very wide base compared with the wild type (left).

per sample (Supplemental Table S1), and single-nucleotide polymorphism (SNP) frequencies were determined between the pooled, sequence-enriched DNA samples and wild-type cv Bowman and visualized in the context of the physical/genetic map of barley (Fig. 2B; Supplemental Fig. S3). In all five pools, an easily traceable shift in overall SNP frequency could be observed at the expected recombination break points determined previously by low-density genotyping (Fig. 2B).

Due to the highly reduced recombination frequency at the genetic centromeres of barley chromosomes, the genetic resolution of barley physical map order was low in this region, and the correct linear order of a large part of the allocated physical map information in this area of the barley chromosomes was rather uncertain. Thus, the immediate identification of a highly resolved and limited physical target interval carrying the *lax-a* locus was not achieved. Consequently, the analysis was modified by categorizing SNPs from the pool sequencing as codominant genotype scores according to the percentage of reads with mutant alleles mapped at the variant site. SNP positions with a frequency of less than 20% mutant reads were scored as the wild-type genotype, those with more than 80% mutant reads were scored as the homozygote mutant, and those between 20% and 80% were scored as the heterozygote genotype. The relaxed thresholds in genotype calls

were implemented due to the risk of false-positive read mappings (e.g. by misidentification of the respective multiplexing index; Kircher et al., 2012) or to avoid the risk of bias in SNP frequencies introduced by less read coverage of targets in one of the pools. This allowed us to filter for SNPs in targets that cosegregate with the respective phenotypic characteristic of each pool independently from the status of anchoring on the physical map (Fig. 2). Those SNPs can be interpreted as cosegregating markers and are expected to be located either within the causal gene itself or in close proximity to it. In total, 15 whole-genome shotgun sequencing (WGS) contigs containing capture targets with SNPs following the required pattern were identified (Supplemental Table S2). Nine high-confidence genes (Supplemental Table S3) were identified by sequence comparison with the barley gene set (Mayer et al., 2012).

Since the *lax-a* mutation was obtained by fast-neutron mutagenesis (Franckowiak and Lundqvist, 2010), which frequently introduces partial or complete gene deletions (Li and Zhang, 2002), we surveyed for targets of the enrichment assay that were not covered by sequence reads in the pools of recombinant plants with the mutant phenotype. If the gene was represented in the target enrichment design and it was deleted (at least partially) due to mutation, no sequence read coverage would be expected for mutant phenotype pools,

Table I. *Physical map positions of genetically mapped markers*

n.a., Not anchored to physical map.

Marker Identifier	Barley High-Confidence Gene[a]	cv Bowman WGS Contig Identifier[a]	Genetic Position[a]	Physical Map Contig[a]	Physical Position[a]
			cM		Mb
1_0974	AK248898.1	contig_201113	17.92	FPC_1748	11,244,320
1_0580	MLOC_68535.2	contig_844634	31.25	n.a.	19,657,720
1_1198	MLOC_3013.1	contig_12040	43.95	n.a.	70,569,640
1_0157	AK251398.1	contig_884009	42.23	n.a.	153,040,800
1_1469	AK358200	contig_895954	42.23	FPC_44251	199,813,600
1_0481	MLOC_22626.1	contig_143316	42.23	n.a.	253,551,480
2_0524	AK356301	contig_221162	42.23	n.a.	248,503,440
HvLax-a	MLOC_61451.6	contig_68343[b]	42.23	FPC_2862	203,930,400
Bd4g43680	MLOC_73193.3	contig_68744	42.23	FPC_3522	259,218,280
1_1260	MLOC_4554.1	contig_881005	44.51	n.a.	283,803,760
2_0239	MLOC_63089.10	contig_271776[c]	42.23	n.a.	264,640,800
2_1148	MLOC_64817.1	contig_1786585[c]	47.5	n.a.	337,184,520
2_0713	MLOC_68788.2	contig_268627	51.45	n.a.	386,809,320

[a]From Mayer et al. (2012).　　[b]Contig was anchored by PCR-based bacterial artificial chromosome (BAC) library screening.　　[c]cv Barke WGS.

whereas wild-type phenotype pools of recombinant plants should exhibit normal (average) read coverage for the respective target enrichment regions. Due to the above-mentioned risk of false-positive read mappings, a maximum read coverage threshold of 2-fold was accepted for pools with mutant phenotype (lax-3 and lax-4). Furthermore, a minimum read coverage of 5-fold was required at similar target sites for wild-type phenotypic pools (lax-1, lax-2, and lax-5). This analysis revealed 12 additional WGS contigs with putative candidate targets (Supplemental Table S4), which were analyzed for genes by sequence comparison with the barley gene set (Mayer et al., 2012). One gene, MLOC_61451.6, was detected that was not covered by sequence reads in the mutant phenotype recombinant pools lax-3 and lax-4, indicating its likely deletion in the *lax-a* mutant (Supplemental Table S5). This gene, therefore, represented a strong candidate gene conferring the *lax-a* phenotype.

Only a few of the 27 WGS contigs identified by the two parallel approaches were already integrated into the physical map framework of barley (Mayer et al., 2012); thus, their physical relationship remained unclear at this stage. We considered synteny between the barley and *Brachypodium* spp. genomes in order to deduce a potential physical order of the genes represented on the respective 27 WGS contigs. Seven out of the 10 putatively orthologous gene models were allocated to a small physical interval (144 kb) in *Brachypodium* spp. The *Brachypodium* spp. ortholog of the potentially deleted barley gene was located in the center of this syntenic block (Fig. 2D).
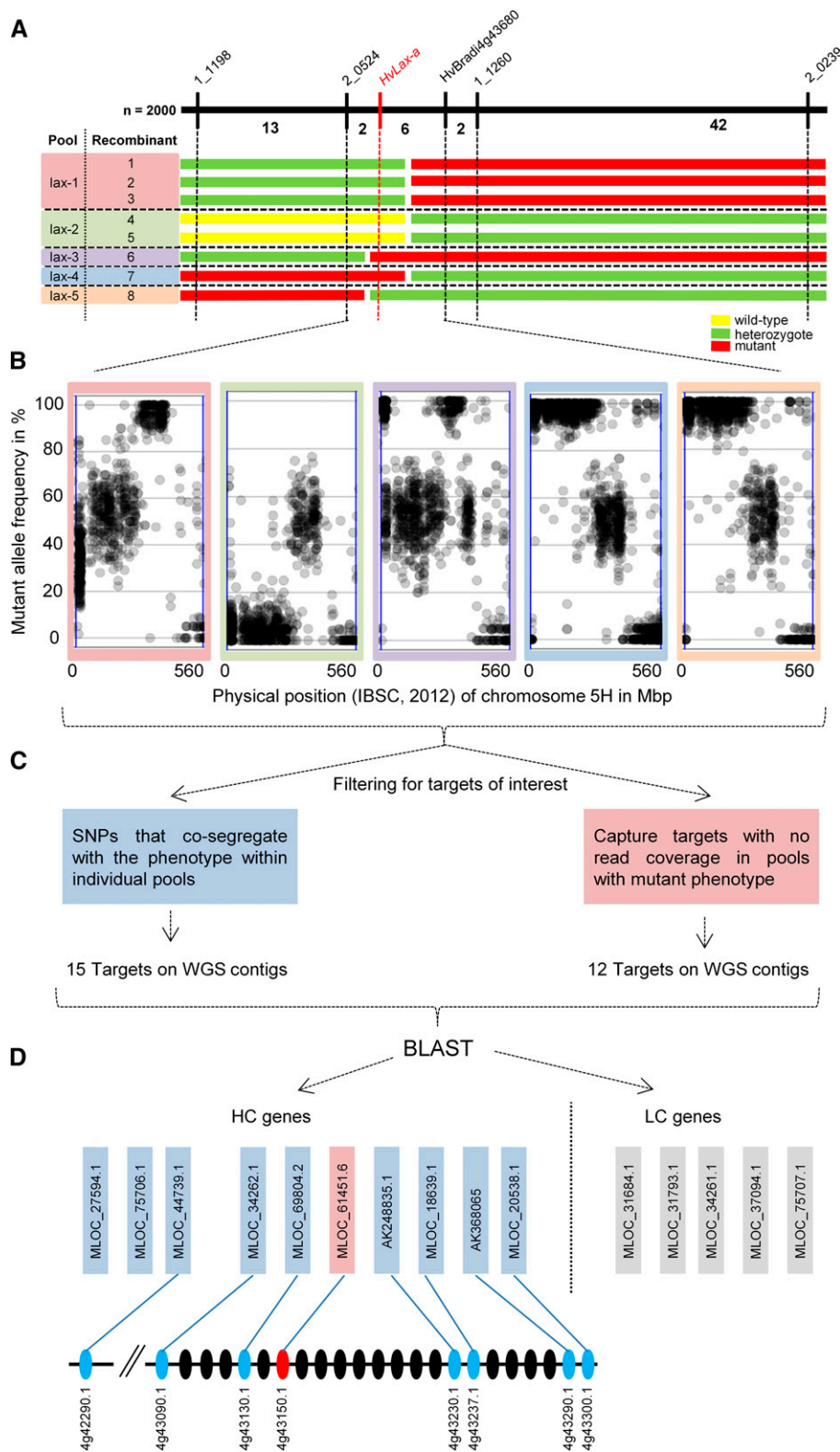
The Gene *HvLax-a* Resides in a 450-kb Deletion in the Mutant BW457

As the WGS contig bearing the candidate gene was not linked to the barley physical map, the candidate gene MLOC_61451.6 was used to PCR screen a barley BAC library, and four clones (HVVMRXALLeA0046E04, HVVMRXALLeA0122D17, HVVMRXALLeA0209O12, and HVVMRXALLeA0379H14), all belonging to the same BAC contig (FPC_2862) of the physical map (Ariyadasa et al., 2014), were identified. A minimum tiling path of overlapping nonredundant BAC clones, spanning the complete FPC_2862, was shotgun sequenced and de novo assembled, yielding 2.3 Mb of unique sequence (Supplemental Table S6). WGS survey-sequencing data of genotypes cv Bowman and mutant NIL BW457 were mapped against the newly generated BAC contig reference sequence. This analysis predicted a deletion of 436/554 kb (minimum/maximum) in the mutant genotype BW457 in the center of FPC_2862 (Supplemental Fig. S4). Based on a previously existing gene annotation (Mayer et al., 2012), four genes were identified on the entire sequenced BAC contig; however, only MLOC_61451.6 was affected by the deletion (Table II; Supplemental Fig. S4; Supplemental Table S7). The candidate gene consists of two exons and a single intron (Fig. 3A). PCR amplification from complementary DNA of cv Bowman was performed to determine splice site positions (data not shown). The predicted coding sequence of MLOC_61451.6 erroneously contained an additional 6 bp that are actually part of the intron.

Mutant Analysis Confirmed the Identification of the Gene *HvLax-a*

In order to test whether the deletion of candidate gene MLOC_61451.6 confers the *lax-a* mutant phenotype, the gene was resequenced in a series of 29 independent *lax-a* alleles in mutant accessions obtained from the Nordic Genome Resource Center (http://www.nordgen.org; Table III). In 14 genotypes, the candidate gene could not be amplified, indicating its complete deletion. The failure of PCR in these cases

Figure 2. Cloning-by-sequencing of the gene *HvLax-a*. A sequence-assisted evaluation of a predefined mapping interval was used to identify candidate genes underlying the *lax-a* phenotype. A, Eight recombinant plants out of 1,970 F2 plants delimited a 0.2-cM mapping interval on chromosome 5H. Marker scores and phenotype scores for each recombinant are represented by a color code for simplification (yellow = wild type, green = heterozygote, and red = mutant). Genotypes with identical marker haplotype/phenotype combinations were pooled for target enrichment resequencing (Mascher et al., 2013a). B, Obtained sequence reads of the individual pools were mapped to the reference cv Bowman (Mayer et al., 2012) for SNP discovery and determination of SNP frequencies. Visualization of SNP frequency plots was restricted to chromosome 5H for each individual pool. The *x* axis shows the physical expansion of chromosome 5H (Mayer et al., 2012), and the *y* axis represents the percentage of mapped reads with alternative mutant alleles from 0% to 100% for each SNP (visualized as dots). C, Filtering for candidates identified 27 targets on WGS sequence contigs. D, Identified high-confidence (HC) and low-confidence (LC) genes (Mayer et al., 2012) on WGS contigs were used for homology analysis and revealed that seven of eight identified putative homolog *Brachypodium* spp. gene models cluster in a small syntenic interval of *Brachypodium* spp.

cannot be attributed to highly polymorphic primer-binding sites due to a putatively diverse haplotype of the genotypic background of these mutants, since the gene could be amplified from independent alleles induced in the same genetic background of cv Bonus, cv Foma, or cv Kristina (Table III). Fourteen accessions carried point mutations; in seven cases, these resulted in the formation of premature stop codons, six resulted

Table II. *Annotated genes located on FPC_2862*

High-Confidence Genes[a]	Annotation[a]	*Brachypodium* spp. Identifer[b]
MLOC_61451.6	NPR1 protein	Bradi4g43150.1
AK373675	Strictosidine synthase family protein	Bradi4g43137.1
MLOC_69804.2	2-Isopropylmalate synthase B, putative	Bradi4g43130.1
MLOC_10658.1	Cytochrome P450	Bradi4g43110.1

[a]From Mayer et al. (2012). [b]Homologous genes in *Brachypodium* spp. predicted by sequence similarity (BLAST).

in nonsynonymous amino acid substitutions, and one resulted in an altered splicing site. One mutant carried two mutations: a 2-bp deletion and a single-base deletion in close proximity, causing a single amino acid deletion and one amino acid exchange (Fig. 3B; Table III). Among the cv Bowman NILs (Druka et al., 2011), an additional accession, BW458, was described to exhibit the *lax-a* mutant phenotype. In this accession, the first part of exon 1 could not be amplified by PCR, again indicating a partial gene deletion (Fig. 3). All analyzed mutant accessions expressed the characteristic *lax-a* phenotype.

In addition to resequencing the existing allelic series of *lax-a* mutants, a population of 7,979 EMS-mutagenized plants (Gottwald et al., 2009) was screened by TILLING. Eighteen mutations leading to nonsynonymous amino acid changes were identified (Supplemental Table S8). A single mutation, C127T (L43F; mutant 8476), revealed the typical *lax-a* phenotype showing five anthers, extended rachis internode length, broadened base of the lemma awn, and uncovered seeds (Supplemental Fig. S5). The respective M3 family was segregating for the mutation, and only the two homozygous mutant M3 plants showed the *lax-a* phenotype, consistent with the recessive nature of the mutated gene. The same mutation was shared by an allele (*lax-a.278*; NGB116503) of the above-described lines from the Nordic Genome Resource Center (Table III). A test for allelism was

performed between the mutant line used for cloning (BW457), the TILLING mutant 8476, and BW458. All F1 plants exhibited the typical *lax-a* phenotypic syndrome (Supplemental Fig. S5), thus confirming the allelic status and further supporting that MLOC_61451.6 is the functional gene underlying the *lax-a* phenotype in the respective barley mutants. Consequently, the gene was named *HvLax-a*.

HvLax-a Is a Homolog to Arabidopsis *BOP1* and *BOP2*

Sequence comparison of *HvLax-a* revealed homology to the Arabidopsis genes *BOP1* and *BOP2*, which together control leaf morphogenesis and flower morphogenesis and promote floral organ abscission (Ha et al., 2004; Hepworth et al., 2005; Norberg et al., 2005; McKim et al., 2008). Both genes belong to a small gene family in Arabidopsis, and gene members carry conserved BROAD COMPLEX, TRAMTRACK, and BRICK À BRACK/POXVIRUSES and ZINC FINGER and ANKYRIN-REPEAT (ANK) domains. The gene family in Arabidopsis includes the genes *BOP1* and *BOP2* as well as the four plant defense-related *NON-EXPRESSOR OF PR GENES1-like* (*NPR1-like*; Hepworth et al., 2005). A combined analysis of these Arabidopsis genes and their respective barley homologs revealed a conserved phylogeny of *BOP* and *NPR1-like* genes in barley (Supplemental Fig. S6). *HvLax-a* and its closest barley paralog, AK360734, represented the putative orthologs of the Arabidopsis genes *BOP1* and *BOP2*. However, the level of sequence conservation between barley and Arabidopsis did not allow us to determine absolutely the orthology relationship between the members of both gene pairs.

HvLax-a and Its Paralogous Gene Affect Different Aspects of Barley Plant Architecture

In Arabidopsis, *BOP1* and *BOP2* have partially redundant functions (Hepworth et al., 2005; Norberg et al., 2005). To test the hypothesis that, in barley,
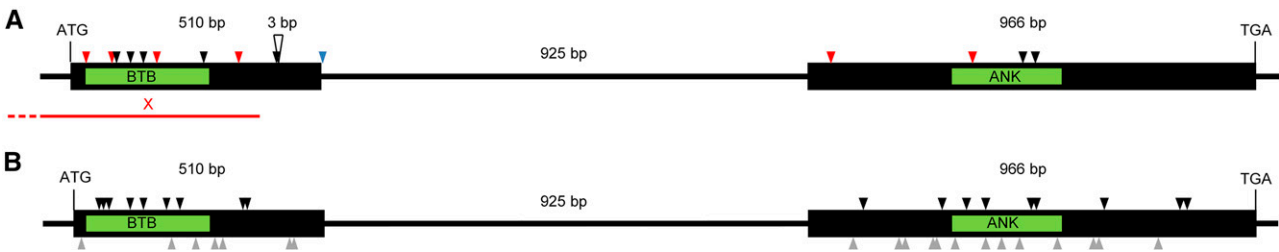

Figure 3. Schematic map of induced mutations in the gene *HvLax-a*. The genomic sequence of *HvLax-a*, consisting of two exons (black boxes) spaced by a single intron (black line), is visualized. Green boxes indicate conserved sequences encoding for the protein domains of BROAD COMPLEX, TRAMTRACK, and BRIC À BRAC (BTB) and ANKYRIN REPEAT (ANK). The distribution of mutant alleles is visualized along the *HvLax-a* gene model for *lax* mutant accessions obtained from the Nordic Genetic Resource Center (http://www.nordgen.org/; A) and targeting induced local lesions in genomes (TILLING) analysis (B). Triangles are color coded according to the effect of the mutation (black = nonsynonymous, gray = synonymous, red = premature stop, blue = altered splicing, and white = deletion). The red line indicates the partial deletion present in cv Bowman NIL BW458 (B).

Table III. *Resequencing of independent lax-a accessions*

Nordic Genome Resource Center Accession No.	Mutant	Mutant Type	Original Cultivar	Mutagen Used
116334	*lax-a.01*	Complete deletion	Bonus	γ rays
116338	*lax-a.4*	C1983T (S348F)	Bonus	Cumarine
116342	*lax-a.8*	Complete deletion	Bonus	Neutrons
116354	*lax-a.20*	Complete deletion	Bonus	Neutrons
116372	*lax-a.37*	Complete deletion	Bonus	Neutrons
116374	*lax-a.39*	Complete deletion	Bonus	X rays
116388	*lax-a.54*	T149C (F50S)	Bonus	Ethylene imine
116426	*lax-a.92*	Complete deletion	Bonus	X rays
116436	*lax-a.208*	Complete deletion	Foma	X rays
116446	*lax-a.218*	A347T (Y116F)	Foma	Ethylene imine
116450	*lax-a.222*	T125A (V42E)	Foma	Ethylene imine
116458	*lax-a.229*	C26A (S9*)	Foma	Glyidol
116483	*lax-a.256*	A1505T (K194*)	Foma	Isopropyl methanesulfonate
116503	*lax-a.278*	C127T (L43F)	Foma	Ethyl methanesulfonate (EMS)
116510	*lax-a.286*	C1853T (Q305*)	Foma	EMS
116560	*lax-a.353*	Complete deletion	Kristina	Neutrons
116579	*lax-a.369*	T512A (altered splicing)	Kristina	Ethylene imine
116608	*lax-a.398*	T461G (L154R), 3-bp deletion (461, 462, 465)	Kristina	γ rays
116613	*lax-a.405*	Complete deletion	Kristina	X rays
116614	*lax-a.406*	Complete deletion	Kristina	Neutrons
116622	*lax-a.413*	T123A (C41*)	Bonus	EMS
116647	*lax-a.434*	Complete deletion	Bonus	Neutrons
116650	*lax-a.437*	T1992A (L331H)	Bonus	Isopropyl methanesulfonate
116659	*lax-a.444*	Complete deletion	Bonus	Neutrons
116664	*lax-a.448*	C184T (Q62*)	Bonus	EMS
116668	*lax-a.450*	G417A (W139*)	Bonus	Sodium azide
116675	*lax-a.455*	G417A (W139*)	Bonus	Sodium azide
116695	*lax-a.472*	Complete deletion	Bonus	X rays
119823	*Naked caryopsis lax Erectoides2*	Complete deletion	Bonus	Neutrons

mutations in the two *BOP-like* genes could result in similar phenotypic alterations, we screened the barley TILLING population to identify functional mutants for *AK360734*. A series of 25 nonsynonymous and 21 synonymous mutations, one premature stop codon (9425_1), and one splice site mutation (13391_1) were identified (Supplemental Table S9). Mutants affected by nonsynonymous amino acid exchanges did not show any obvious phenotypic effect. The two mutants affected either by a premature stop codon or a splice site mutation, respectively, exhibited a liguleless phenotype with irregular outgrowth of auricles (Supplemental Fig. S7, D–F) and produced fewer than three tillers (Supplemental Fig. S7, B and C). M3 families segregated for the mutation with perfect linkage of homozygous mutant genotype and the described phenotypic alterations. Phenotypic effects were severe (stunted growth, strong curling of the shoot and leaves), and only five out of 15 homozygous mutant plants grew to maturity (four plants of M2 family 9425_1 and one plant of M2 family 13391_1). None of the plants showed any characteristic *lax-a* changes. The observed phenotypic syndrome resembled exactly a pattern reported previously for the barley mutant *uniculme4* (*cul4*; Tavakol et al., 2015). Indeed, when completing our TILLING analysis of *AK360734*, the same gene was reported as the

underlying factor of the *cul4* phenotype (Tavakol et al., 2015). Our analyses, therefore, provided independent confirmation of these findings.

Natural Variation of *BOP-like* Genes in Barley

HvLax-a and its paralog *HvCul4* are involved in regulating two major agronomically relevant traits, tiller number and spike morphology. Thus, natural alleles of both genes could have been under selection during barley domestication, adaptation, or more recent breeding. To test this, we investigated the natural diversity for both barley *BOP-like* genes *HvLax-a* and *HvCul4*. The open reading frame (ORF) of both genes was amplified in a set of 83 wild barley (*Hordeum spontaneum*) lines and 222 domesticated barley lines consisting of landraces and improved cultivars (Supplemental Table S10). The majority of accessions (205; 67%) carried one major haplotype for *HvLax-a*, and the remaining genotypes belonged to nine minor haplotypes specified by 11 polymorphic sites consisting of nine synonymous and two nonsynonymous changes (Fig. 4; Table IV). For *HvCul4*, a significantly higher number of polymorphic sites and a more diverse haplotype structure were revealed (Fig. 4). The 48

polymorphic sites were represented by 38 synonymous and 10 nonsynonymous SNPs (Table IV). In addition, some accessions carried a 3-bp (domesticated material) or 6-bp (wild material) insertion within the second exon of *HvCul4*. The *HvLax-a* and *HvCul4* haplotype diversity was decreased by about 88.2% (from 0.6644 to 0.0781) and 18.7% (from 0.9412 to 0.765) in domesticated versus wild barley, respectively. Nucleotide diversity was reduced as well for *HvLax-a* (from 0.0009 to 0.0005) but, in contrast, was increased slightly for

HvCul4 (from 0.00456 to 0.00493) between wild and domesticated material (Table IV). The Tajima D test (Tajima, 1989) for neutrality of DNA polymorphisms was performed to determine if the observed changes in polymorphisms were likely caused by a nonrandom shift or by natural selection. None of the calculated Tajima's D values reached significance ($P < 0.1$); thus, the observed changes in sequence diversity were considered unlikely to be functions of selection of the two analyzed genes.
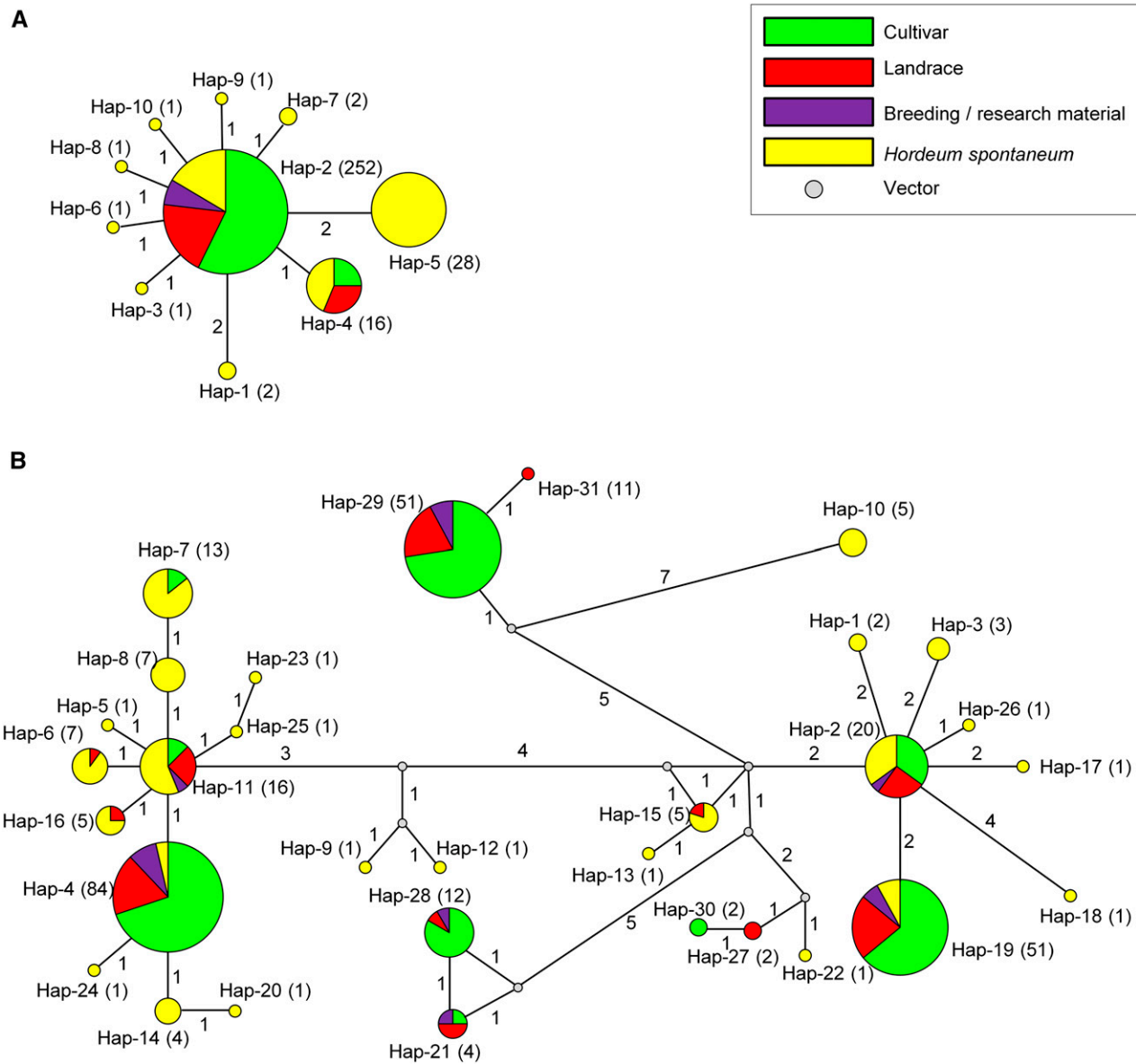

Figure 4. Diversity analysis of *HvLax-a* and *HvCul4*. Median-joining networks were derived from haplotypes identified by resequencing the ORF of *HvLax-a* (A) and *HvCul4* (B) in 83 *H. spontaneum* accessions (yellow), 55 barley landraces (red), 150 barley cultivars (green), and 17 accessions of breeding/research material (purple). Haplotypes were labeled with haplotype identifiers and numbers of accessions sharing the respective haplotype (parentheses). Circle sizes are proportional to the number of accessions per haplotype. Lengths of connector lines refer to the number of nucleotide substitutions between haplotypes (numbers on connecting lines = the number of mutations).

Table IV. *Statistics from the diversity analysis of HvLax-a and HvCul4*

Parameter	HvLax-a			HvCul4		
	Wild	Domesticated	All	Wild	Domesticated	All
No. of haplotypes	10	2	10	26	13	31
Haplotype diversity	0.6644	0.0781	0.307	0.9412	0.765	0.8582
No. of sites	1,476	1,476	1,476	1,548	1,545	1,551
No. of sites (gaps excluded)	1,476	1,476	1,476	1,542	1,542	1,542
Nucleotide diversity	0.0009	0.00005	0.00034	0.00456	0.00493	0.00499
Polymorphic sites	11	1	11	44	27	48
Synonymous	9	1	9	34	24	38
Nonsynonymous	2	/	2	10	3	10
Tajima's D	−1.06982	−0.53007	−1.61662	−0.70735	1.72692	−0.03471

Phylogenetic Analysis of the *BOP-like* Genes

A sequence database screen in a previous study revealed the existence of two to three *BOP-like* genes in most plant species (Khan et al., 2014). Sequence conservation between Arabidopsis *AtBOP1* and *AtBOP2* and barley *HvLax-a* and *HvCul4* did not allow defining their orthology relationship. Therefore, we extended the phylogenetic analysis to a larger number of angiosperm, fern, and moss species to better reveal the evolutionary relationships between gene family members and support hypotheses of putative functional orthology. A maximum likelihood-based phylogenetic tree was constructed based on protein sequences. This analysis showed that, despite the existence of multiple BOP homologs in mosses and ferns, the gene family members in higher land plants were unlikely to have evolved directly from these evolutionarily distant copies (Supplemental Fig. S8). The analyses did not allow us to determine which nonangiosperm *BOP-like* gene was conveyed to younger angiosperms. Recently, based on the higher sequence conservation of dicot *BOP-like* genes, it was proposed that they may have originated from more recent duplication events than the monocot genes. This may go some way toward explaining the functional redundancy of the Arabidopsis genes (Tavakol et al., 2015). The *BOP-like* genes in the Poaceae showed a unique pattern of diversification compared with the other analyzed, exclusively dicot, *BOP* families. While the *HvCul4*-containing clade was closely related to all BOP-like members of dicot plant families, the *HvLax-a*-containing clade was more distinct. One may conclude that *HvCul4* is orthologous to either *BOP1* or *BOP2*. *HvLax-a* (and the respective orthologs of other Poaceae members), however, was either a direct but more diversified *BOP1/2* ortholog or originated as a Poaceae-specific gene duplication followed by neofunctionalization/subfunctionalization leading to higher sequence diversity. As members of the *NPR1-like* gene family, *HvLax-a* and *HvCul4* may play a role in defense responses and jasmonate signaling, as has been shown for the Arabidopsis *BOP* genes. These putative additional functions may have acted as additional factors influencing the evolutionary history of these genes (Canet et al., 2012; Khan et al., 2015).

DISCUSSION

Mutation of *HvLax-a* causes pleiotropic phenotypic aberrations in the barley inflorescence, including an elongated spike rachis, homeotic conversion of lodicules into stamenoid structures, thin and angular grains exposed at spike maturity due to the reduced width of palea and lemma, and a broadened base of the lemma awn. The functional gene, *HvLax-a*, resides in the pericentromere area of barley chromosome 5HL, a region characterized by very low recombination frequency. It was identified after deploying an innovative strategy of mapping-by-sequencing and cloning-by-sequencing as a homolog of the transcriptional regulator genes *BOP1* and *BOP2* of Arabidopsis.

HvLax-a, a Key Regulatory Gene of Barley Inflorescence Architecture

HvLax-a showed strong sequence homology to the *AtBOP1/2* genes, which in Arabidopsis are expressed in lateral organ boundaries and redundantly regulate the proximal and distal growth of leaves, the floral transition, and organ identity (Ha et al., 2004; Hepworth et al., 2005; McKim et al., 2008). Single loss-of-function mutants in Arabidopsis showed no or very weak phenotypic effects, whereas double mutants were severely affected in growth (Hepworth et al., 2005; Norberg et al., 2005). Florets of *AtBOP1/2* mutants exhibited a loss of floral organ abscission and changes of symmetry in conjunction with the formation of extra floral organs, with fused organs often appearing on the abaxial site of florets (Hepworth et al., 2005). In barley, *lax-a* florets did not exhibit supernumerary organs, but lodicules were homeotically transformed into stamenoid organs and an ectopic growth of the bases of the lemma awn was observed. The leaf alterations in Arabidopsis *bop1/2* mutants more closely resembled the phenotypic effects in mutants of the second barley *BOP-like* gene, the *cul4* mutant (Tavakol et al., 2015). *HvCul4* was shown to control the number of tillers, ligule development, and proximal-distal leaf patterning. Interestingly, in barley, loss-of-function mutation even of a single *BOP-like* gene resulted in the respective phenotypic alterations. Complete loss of *HvLax-a* did not result in any obvious effect on leaf composition or tillering, and deletion of

HvCul4 did not impact spike architectural traits. The differences between Arabidopsis and barley may be the result of increasingly specific subfunctionalization of *BOP1/2* homologs in barley, a hypothesis that will require further testing by, for example, analyzing the phenotypic characteristics of *lax-a/cul4* double mutants. Further support for this hypothesis is provided by the publicly available expression data of eight different plant tissues of barley (Mayer et al., 2012). Both genes showed a partially overlapping expression pattern but distinct expression maxima, which are consistent with the notion of different physiological roles of both genes (Tavakol et al., 2015). *HvCul4* expression levels were highest in young embryos of germinating seeds and developing tillers, while *HvLax-a* transcript abundance reached its maximum in developing spike meristems (Supplemental Fig. S9). We know from an RNA sequencing experiment (own unpublished data [M. Jost and N. Stein]; data not shown) from different stages of immature spike meristems that misexpression of *HvLax-a* in *lax-a* mutants does not influence *HvCul4* expression, which would support the hypothesis of independent regulation of *BOP-like* genes in barley.

To our knowledge, *HvLax-a* and *HvCul4* are the first *BOP-like* genes characterized in detail in monocot species, and as a result, the underlying regulatory networks of *BOP-like* genes remain largely unknown. The observed phenotypic similarities between *BOP-like* mutants in barley and Arabidopsis could indicate at least a partially conserved function. In Arabidopsis, the *BOP1/2* regulatory network has been explored extensively. *BOP1/2* act in organ boundaries and control meristem activity by regulating the expression of *KNOTTED-like* homeodomain (*KNOX*) and *BEL1-like* homeodomain (*BELL*) gene family members, which belong to the three-amino-acid-loop-extension class of proteins. In Arabidopsis, these genes are important for meristem maintenance and organ differentiation (for review, see Hamant and Pautot, 2010; Khan et al., 2014). *AtBOP1/2* promote the expression of the lateral organ boundary domain gene *ASYMMETRIC LEAVES2* (*AS2*), which forms a complex with *AS1* to suppress the expression of the *KNOX* genes *BREVIPEDICELLUS* (*BP*), *KNAT2*, and *KNAT6* in leaves (Jun et al., 2010). In contrast, the opposite mode of regulation has been reported to control inflorescence stem elongation. The *BP* and *BELL-like* homeodomain gene *PENNYWISE* functions as a repressor of *BOP1/2*, *KNAT6*, and the *BELL* gene *ARABIDOPSIS THALIANA HOMEOBOX1* (*ATH1*), while *BOP1/2* activate *KNAT6* and *ATH1* in a shared pathway (Khan et al., 2012a, 2012b, 2015) Recently, it was shown that *BOP1/2* function as negative regulators of the bZIP transcription factor (TF) FD, which is a component of the floral transition pathway of *FLOWERING TIME LOCUS T* (*FT*) and is required for the activation of the key floral development regulatory genes *LEAFY* (*LYF*) and *APETALA1* (*AP1*; Andrés et al., 2015). Opposing roles for *BOP1/2* were proposed in later stages of floret development via directly promoting the expression of *AP1* and *LYF*, thus controlling

floral organ patterning (Karim et al., 2009; Xu et al., 2010; Andrés et al., 2015).

As the role of *KNOX* genes in plant development is conserved between dicots and monocots (Hay and Tsiantis, 2010), the reported *BOP1/2*-dependent *KNOX* gene regulation in Arabidopsis could indicate similar activity in monocots. As an example, mutations in *HvKNOX3* lead to the *Hooded* phenotype in barley, where an extra floret is formed on the lemma at the transition zone between the leafy part and the awn (Müller et al., 1995). The *lax-a* characteristic broadening at the base of the awn could indicate an incomplete version of such a transition and, thus, point at *HvBOP-like* and *HvKNOX* gene interaction.

In rice (*Oryza sativa*), a relatively close relative of barley, the TF of the *JAGGED LATERAL ORGANS* and the *YABBY* TF family have been reported as regulators of *KNOX* gene expression in rice panicles. Both TF classes regulate *KNOX* gene expression in a shared pathway together with *AtBOP1/2* and are repressed in Arabidopsis leaves and bracts (Norberg et al., 2005; Ha et al., 2007; Jun et al., 2010). Mutations of members belonging to these TF families are associated with changes in the spatiotemporal expression of *KNOX* genes causing pleiotropic alterations in the rice inflorescences: (1) elongated panicles (Horigome et al., 2009); (2) reduced growth of the lemma and palea; and (3) alterations in the number and identity of floral organs (Horigome et al., 2009; Xiao et al., 2009; Tanaka et al., 2012). These analogies in rice and barley anatomy and the similarities in the regulatory networks among rice and Arabidopsis may again imply that *BOP* gene regulatory pathways are partially conserved between monocot and dicot plants, suggesting that the barley *BOP-like* gene *HvLax-a* could fulfill a central function in controlling meristem identity, as *BOP1/2* does in Arabidopsis.

In addition to their potential effect on *KNOX* gene regulation, *BOP* genes in barley also may be involved in the regulation of the MADS box TF. In Arabidopsis, *BOP1/2*-regulated expression of *AP1* leads to the downregulation of *AGAMOUS-LIKE24*, a homolog of *AGAMOUS* (*AG*; Xu et al., 2010). Ectopic expression of *OsMADS3*, the rice ortholog of *AG* (Kyozuka and Shimamoto, 2002), leads to the homeotic transformation of lodicules into stamens. Therefore, the conversion of lodicules into stamens in *lax-a* could potentially be explained by a lack of *AG* down-regulation in lodicules. While there is some support for such speculation, further experiments, such as quantitative transcriptional profiling of microdissected immature spike meristems, will be required to conclusively demonstrate the postulated role of *HvLax-a* and *HvCul4* in *KNOX* and *MADS* box gene regulation in barley.

Natural Diversity Analysis

Since *HvLax-a* and *HvCul4* are regulators of agronomically important traits such as spike morphology and tiller number, we explored whether the sequences

of both genes in barley accessions collected from different environmental and geographical origins revealed putative signatures of selection during early or recent barley adaptation or improvement. *HvLax-a* exhibited a very low level of diversity, even in wild barley accessions. Since the complete deletion of *HvLax-a* is not lethal and most nonsynonymous mutations did not induce any visible phenotype in greenhouse-grown plants, it was somewhat unexpected to find such a low level of natural sequence diversity. We believe that this was unlikely to be the result of purifying selection of *HvLax-a* and was more likely a direct consequence of its location in a low-recombining chromosomal region; as nucleotide diversity is correlated with recombination rate, it is generally reduced in the low-recombining genetic centromeres (Begun and Aquadro, 1992). In these regions, extensive linkage disequilibrium to other, yet to be identified, factors under strong selection could have led to the fixation of *HvLax-a* already in the wild barley gene pool.

In contrast, *HvCul4* showed high nucleotide diversity relative to *HvLax-a*. The diverse *HvCul4* haplotype network could not be explained by any known population structure in the analyzed panel (Haseneyer et al., 2010; Pasam et al., 2012) for row type and geographic origin, since all the major haplotypes contained both two- and six-row barley lines and could not be attributed to specific regional adaptation concerning latitude/longitude coordinates. *HvCul4* nucleotide diversity in domesticated barley accessions was increased slightly compared with wild barley, although estimates of Tajima's D in cultivars, landraces, and wild barley failed to reach significance. We conclude that differences in nucleotide diversity were most likely caused by random bottleneck effects characteristic of the analyzed population. Extending this analysis to a larger number of accessions as well as to the flanking genomic region would be required to reach more definitive conclusions.

Among the identified polymorphisms in *HvCul4*, premature stop codons and splice site mutations that would have major negative impacts on protein function were not observed. Although we did not characterize the accessions for phenotypic variations, we do not expect an overly negative impact of the identified nonsynonymous polymorphisms, since they were located exclusively outside of the putative functional domains. Even under greenhouse conditions, *HvCul4* TILLING mutants exhibited phenotypic changes with severe negative effects on fitness. Thus, although higher sequence diversity was observed when compared with *HvLax-a* in our panel of genotypes, it is likely that severely affected alleles would be under strong negative selection in natural populations. Consequently, the molecular variation we observed revealed no indication of an active selection process for either gene during domestication, adaptation, and improvement. It seems more likely that the patterns of diversity we observed are simply a product of the contrasting genomic environments in which either gene resides.

Cloning-by-Sequencing in Barley: Does Genomic Position Matter?

Forward genetics has been feasible, but labor intensive, in barley for several years (Stein and Graner, 2005). Based on bulked segregant analysis (Michelmore et al., 1991), mutation identification by high-throughput sequencing was established recently in Arabidopsis (for review, see Schneeberger and Weigel, 2011) and was extended to barley by combining the approach with target enrichment resequencing (Mascher et al., 2014). Cloning-by-sequencing of barley *MANY NODED DWARF* was exceptionally successful, but it was largely enabled by the location of the gene in a recombination hotspot. Here, we applied a modified approach to clone the gene *HvLax-a*, necessitated by its location in a region of highly suppressed recombination. We found that it was critical to select highly informative recombinants by high-resolution genetic mapping and pool these for bulked segregant analysis sequencing. Two additional features facilitated *HvLax-a* identification: the target gene was included in the target enrichment assay, and the mode of mutagenesis resulted in complete deletion of the functional gene. As the barley genome sequence was largely an unordered draft (Mayer et al., 2012; Ariyadasa et al., 2014), our initial genetic analysis revealed a large physical region of the chromosome represented by highly fragmented sequence information that required a substantial amount of further work to fully resolve. In the near future, the cloning of genes in the nonrecombining part of barley chromosomes will become much more efficient, given the impending release of a highly improved physical map-based reference sequence. This is both timely and important, since a long history of barley mutant research has resulted in well-characterized and easily accessible mutant collections in managed gene banks (Lundqvist, 2009). A large number of mutants chosen to represent the morphological and developmental variation observed in the species have been backcrossed into a single isogenic background of cv Bowman that have already been genetically characterized in some detail (Druka et al., 2011). They represent a valuable resource for systematic gene isolation by mapping-by-sequencing and/or cloning-by-sequencing approaches in the immediate future.

CONCLUSION

In this study, we identified *HvLax-a*, a homolog of Arabidopsis *BOP1/2* genes, that is involved in inflorescence development in barley. The paralogous gene, *HvCul4*, independently controls the leaf blade-to-sheath boundary formation and tillering. *BOP1/2* gene regulatory networks have been explored extensively in Arabidopsis. The identification of paralogous genes in barley revealed both conserved and divergent functions in dicot and monocot plant species. The comparative analysis of the underlying regulatory networks will be greatly facilitated in the future due to the cloning of both *BOP-like* genes of barley. Cloning of the *Lax-a*

gene might open future perspectives in plant breeding, provided that adverse phenotypic effects can be moderated or eliminated. *Lax* florets can open without the impetus force of lodicules, which were reported previously to be essential for open flowering in barley (Nair et al., 2010). Since the wild-type structures of the lemma and palea help keep barley flowers closed during anthesis, the open-flowering *lax-a* phenotype may help to achieve open flowering independent of lodicules to facilitate hybrid breeding in barley. Furthermore, and similar to the effect of the *nud* gene, the mostly hull-less *lax-a* seeds should be preferred for the human food supply (Taketa et al., 2008). The relaxed spike architecture should be beneficial in humid growing conditions to discourage fungal growth and to achieve robust dry seeds for mechanical harvest.

MATERIALS AND METHODS

Plant Material

For genetic mapping, the Arabidopsis (*Arabidopsis thaliana*) NIL BW457 (Druka et al., 2011), bearing an introgressed segment with the fast-neutron-induced *lax-a.8* mutant allele (Franckowiak and Lundqvist, 2010), was backcrossed to the recurrent parent cv Bowman to generate an F2 population.

For mutant analysis, additional *lax-a* mutant accessions were investigated. Besides the cv Bowman NIL BW457, used for mapping the *lax-a.8* locus, line BW458 was described to exhibit the five-stamen phenotype (Druka et al., 2011). In addition, 29 *lax-a* accessions (Table III) were available from the Nordic Genetic Resource Center (http://www.nordgen.org). All plant material was cultivated under greenhouse conditions (18°C/16°C day/night temperatures). Natural light as well as additional sodium lamps were used for illumination.

Two hundred twenty-two accessions from a preexisting worldwide spring barley (*Hordeum vulgare*) collection (Haseneyer et al., 2010), consisting of 149 improved varieties and 57 landraces plus additional various breeding or research stocks, were used for the analysis of natural diversity. Additionally, 83 wild barley (*Hordeum spontaneum*) accessions from the Near East, Europe, and Asia were analyzed (Supplemental Table S10).

Mutant Analysis

A TILLING population of 7,979 preexisting EMS-treated plants of cv Barke (Gottwald et al., 2009) was screened for independent mutant alleles of *HvLax-a*. Two primer pairs were used to amplify the full ORF (HvLAX_EX1_F/R and HvLAX_Ex2_F/R; Supplemental Table S11) by standard PCR with a final heteroduplex step as described earlier (Gottwald et al., 2009). PCR products were digested with the DNF-480-3000 dsDNA Cleavage Kit and analyzed using the DNF-910-1000T Mutation Discovery 910 Gel Kit on the AdvanCE FS96 system according to the manufacturer's guidelines (Advanced Analytical). Identified SNPs were confirmed by Sanger sequencing (see below). All mutants carrying nonsynonymous SNPs were addressed for phenotyping. The genomic sequences of *HvLax-a* of independent *lax-a* accessions was generated by PCR amplification and subsequent Sanger sequencing to identify sequence variations. The Bowman NILs BW457 and BW458 were amplified by PCR with four primer combinations: HvLAX-F/R1, HvLAX_F/R2, HvLAX_F/R3, and HvLAX_F/R4. The *lax-a* mutant accessions from the Nordic Genetic Resource Center were analyzed by PCR amplification of primer combinations (HvLAX_F/R_7 to HvLAX_F/R_11; Supplemental Table S11). Mutant line lax-a.373 (NGB116583) was excluded from the analysis because of missing the additional stamen phenotype.

Allelism Test of Independent *lax-a* Mutant Alleles

The cv Bowman NIL BW457 was used as the female parent and crossed with TILLING mutant 8476 and NIL BW458. A codominant SNP marker test for heterozygosity was performed to confirm the success of the cross. Since *HvLax-a* was identified to be located within a large deletion, two flanking polymorphic

SNPs, located on FPC_2862 outside of the deletion, were used to genotype the cross of BW457 and BW458 (Supplemental Table S12). Two primer combinations (Supplemental Table S11) were used to amplify these polymorphic SNPs (Supplemental Table S12), and all analyzed F1 plants proved to be heterozygous for both markers. All 16 F1 plants displayed a *lax-a* characteristic phenotype (Supplemental Fig. S5, R–V). For the second cross, between BW457 and the TILLING mutant 8476, only the SNPs on cv Bowman FPC_129575 could be utilized for codominant genotyping (Supplemental Table S12). To generate a second independent confirmation, the first exon was amplified (HvLAX_F/R4; Supplemental Table S11) in all F1 plants as the dominant marker and the fragment obtained was sequenced. All fragments carried the homozygous mutant allele (T) at position 127 bp, transferred from the male parent TILLING mutant 8476. In total, six F1 plants were analyzed for the cross between BW457 and TILLING mutant 8476. All were heterozygous and showed the laxatum-characteristic phenotype (Supplemental Fig. S5, M–Q).

Phenotypic Analysis

F2 plants and F3 progeny of recombinant plants were visually inspected for (1) width of the lemma awn base, (2) exposure of the mature caryopsis, and (3) number of anthers after heading. Average rachis internode length was calculated by dividing the overall ear length of mature spikes by the number of nodes per spike at full maturity (Supplemental Fig. S1).

Histological Analysis

For histological analysis, spikelets were fixed with 4% (v/v) formaldehyde in 50 mM phosphate buffer for 16 h at 8°C. After dehydration in a graded ethanol series, probes were infiltrated and embedded in Spurr's resin. Semithin (1-μm) sections were cut on a Reichert-Jung Ultracut S (Leica), stained with Crystal Violet, and examined with an Axioimager light microscope (Carl Zeiss).

Preparation of Genomic DNA

Plant material for DNA isolation was harvested from greenhouse-grown plants at the three-leaf stage. For genetic mapping, a rapid 96-well plate format DNA isolation on the Biorobot 3000 (Qiagen) system with the MagAttract 96 DNA Plant Core Kit was performed according to the manual (Qiagen). Genomic DNA for exome capture was isolated using a modified cetyl-trimethyl-ammonium bromide method (Stein et al., 2001). Genotyping of TILLING families was performed by DNA extraction according to a modified cetyl-trimethyl-ammonium bromide protocol of Doyle and Doyle (1990). Volumes of reagents were adjusted to 1.2 mL to accommodate a 96-well format with Collection Microtubes (Qiagen).

PCR Amplification

PCR was performed on the GeneAmp PCR System 9700 (Applied Biosystems). A standard touchdown PCR profile was used for all PCR analyses containing two cycling steps: initial denaturation for 15 min at 95°C, followed by 10 cycles of denaturation at 95°C for 30 s, annealing at 60°C for 30 s (decreasing by 0.5°C per cycle), and by extension at 72°C for 60 s; this was followed by 35 cycles of denaturation at 95°C for 30 s, annealing at 55°C for 30 s, and extension at 72°C for 60 s, followed by a final extension step at 72°C for 7 min. PCR products were resolved on 1.5% (w/v) agarose (Invitrogen) gels by electrophoresis.

Genotyping and Map Construction

Marker development for genetic mapping of *HvLax-a* followed a two-stage procedure. Initially, publicly available marker resources based on the previously defined approximately 30-cM introgressed segment for NIL BW457 (Druka et al., 2011) were evaluated. Since BW457 was crossed again with their recurrent parent cv Bowman, we could directly utilize polymorphic SNPs for mapping using underlying sequence information (Close et al., 2009) to convert the array-based marker into a PCR-based cleaved amplified polymorphic sequence marker (Konieczny and Ausubel, 1993) for low-resolution mapping (Supplemental Table S13). Restriction digestion was performed according to the manufacturer's guidelines in a thermo cycler. SNPs used for low-resolution mapping were converted to an eight-plex SNaPshot marker assay for screening an extended mapping population. Extension oligonucleotides are differentiating in size between 30 and 74 bp (Supplemental Table S14). First, amplification of 92- to

227-bp fragments was performed by a multiplex PCR (two reactions; Supplemental Table S14) using standard PCR conditions (see above). PCR cleanup (removal of unincorporated deoxyribonucleotide triphosphates) was achieved by incubation with shrimp alkaline phosphatase and exonuclease 1 (Affymetrix). Reaction conditions as well as subsequent steps of sample preparation were performed according to the supplier's protocol for the ABI PRISM SNaPshot Multipex Kit (Applied Biosystems). Capillary electrophoresis was performed on the Applied Biosystems 3730/3730xl DNA Analyzer equipped with 50-cm capillaries, POP-7 Polymer matrix, and Data Collection Software 3.0 (Applied Biosystems). The system was calibrated with Matrix Standard Set DS-02 (Set E5) according to a user bulletin (Applied Biosystems). Peak histogram analysis for genotyping was done with GenMapper4.0 (Applied Biosystems) software. The second source for marker development was based on known SNPs delivered from WGS survey sequencing of BW457 (see below). JoinMap version 4.0 (Kyazma) was used with the Kosambi mapping function to construct a linkage map.

Sanger Sequencing

PCR amplicons were purified with NucleoFast 96 ultrafiltration plates (Macherey-Nagel). Original PCR primers were used for sequencing using the BigDye Terminator version 3.1 Ready Reaction Cycle Sequencing Kit (Applied Biosystems) on the 3730xl DNA Analyzer (Applied Biosystems). PHRED 20 quality (Ewing and Green, 1998; Ewing et al., 1998) trimmed sequences were analyzed with Sequencher 5.2.3 software (Genecodes).

WGS

Sequencing library preparation was performed according to standard protocols (Mayer et al., 2012). BW457 was sequenced to 8-fold coverage using the Illumina HiSeq 2000 platform (Illumina). Sequence reads were mapped against the cv Bowman WGS assembly (Mayer et al., 2012) with BWA version 0.5.9 (Li and Durbin, 2009). SNP calling was performed with SAMtools version 0.1.17 (Li, 2011) using default parameters.

Exome Sequencing

DNA was quantified with a Qubit 2.0 Fluorometer (Invitrogen), and genotypes with shared marker haplotype/phenotype combinations were pooled to equal amounts before sequence library preparation. One microgram of DNA was fragmented to a range of 200 to 400 bp by ultrasound using the Covaris S220 device with the following settings: 175-W peak incident power, duty factor 10%, 200 cycles per burst, and 100-s treatment time. Sample preparation was done with the Illumina TruSeq DNA Sample Preparation Kit based on the manufacturer's instructions. Different samples or pools were individually indexed and captured together by a single liquid array capture assay (Mascher et al., 2013a; Himmelbach et al., 2014). Sequences of recombinant pools were mapped against the whole-genome shotgun assembly of cv Bowman with BWA 0.5.9 (Li and Durbin, 2009) using the parameter -q 15 for quality trimming. Multisample SNP calling was performed with SAMtools 0.1.19 (Li, 2011) using the command mpileup -q 10 -C50. SNP calls were filtered for coverage and genotype score with a custom script adapted from ProtonGBSPaper (Mascher et al., 2013b). Read depth in capture targets was calculated with BEDtools (Quinlan and Hall, 2010). Genotype calls and coverage values were loaded into the R statistical environment and queried for segregation patterns identical to *lax-a* with custom scripts.

BAC Sequencing

We sequenced selected, physically overlapping BAC clones that represented the complete extension of the BAC contig (FPC_2862) on the Illumina MiSeq system (Supplemental Table S6). Multiplexed library preparation sequencing on the Illumina HiSeq 2000 was performed based on published protocols (Beier et al., 2015).

Physical Anchoring and Deletion Detection

Physical anchoring was performed by PCR-based screening of two independent gene fragments of *HvLax-a* (HvLAX_F/R1 and HvLAX_F/R3; Supplemental Table S11) of multidimensional BAC pools (customized arrangement by Amplicon Express) of the library HVVMRXALLeA (Schulte et al., 2011). In silico anchoring was done by manual inspection of BLASTN hits

(Altschul et al., 1990) of sequenced BACs against physically anchored barley WGS contigs (Mayer et al., 2012).

The WGS data produced for mutant NIL BW457 (see above) were used to predict the size of the deletion. The fact that the sequenced BAC clones were generated from cv Morex meant that a less stringent read mapping was required, which allowed a small percentage of mismatches. In consequence of the short read length (2×100 bp paired-end sequencing), an overrepresentation of highly similar short sequence reads is expected by mapping an entire genome against a short BAC contig, which would most likely lead to distorted read coverage. Therefore, we used the available 1.8-Gb sequence assembly of cv Bowman (Mayer et al., 2012) as a reference for mapping. The average read coverage for each cv Bowman WGS contig was calculated for the respective mapping of mutant and wild-type reads. Sixty-four sequence contigs of this WGS assembly of cv Bowman, representing a cumulative length of 211 kb, were assigned along the sequenced FP contig by BLAST (alignment length $\geq$ 500; identity $\geq$ 99.5%). Seventeen of these WGS contigs, with a cumulative length of 53 kb, showed no sequence coverage by reads from the WGS assembly of the mutant NIL BW457 but the expected coverage of approximately 30-fold from the wild-type cv Bowman reads. All of these contigs were located in the central part of the sequenced FPC_2862 and were used to determine the deletion size (Supplemental Fig, S4).

Haplotype Analysis

In order to study natural genetic diversity, the coding sequence was amplified from 303 genotypes (Supplemental Table S10) using three primer combinations for *HvLax-a* (HvLAX_F/R4, HvLAX_F/R5, and HvLAX_F/R6; Supplemental Table S11) and *HvCul4* (HvCUL4_F/R1, HvCUL4_F/R2, and HvCUL4_F/R3; Supplemental Table S15). All fragments were verified using a forward and reverse Sanger sequencing reaction. A haplotype analysis was performed based on resequencing data of the complete ORFs. Sequence alignments were performed with ClustalW2 (http://www.ebi.ac.uk/Tools/msa/clustalw2/). The DnaSP software package (Librado and Rozas, 2009) was used for haplotype detection under consideration of gaps. DNA ALIGNMENT 1.3.1.1 (http://www.fluxus-engineering.com) was used to produce the .rtf input file for the NETWORK 4.6.1.2 software (http://www.fluxus-engineering.com) to generate a median-joining network (Bandelt et al., 1999).

Phylogenetic Analysis

The protein sequence homology search of HvLax-a was performed by BLASTP (Altschul et al., 1990) against the barley high- and low-confidence gene set (Mayer et al., 2012) to identify paralogous genes in barley. To identify all *BOP-like* members within the plant kingdom, the National Center for Biotechnology Information protein (http://www.ncbi.nlm.nih.gov) and Phytozome version 10.2 (http://phytozome.jgi.doe.gov) databases were surveyed. To test the presence of conserved protein domains in identified candidate protein sequences, a conserved sequence search was performed at the National Center for Biotechnology Information (http://www.ncbi.nlm.nih.gov/Structure/cdd/wrpsb.cgi). Multiple protein sequence alignment was performed using MUSCLE (Edgar, 2004a, 2004b). The phylogenetic analysis was performed using MEGA6 software (Tamura et al., 2013) following the published protocol (Hall, 2013). The maximum likelihood tree was constructed using the JTT model with discrete Gamma distribution and nearest neighbor interchange by applying 1,000 bootstrap replicates. Default program settings were used. An unrooted tree was drawn to scale based on amino acid sequence substitution rate per site.

Illumina exome sequencing data have been deposited at EMBL-ENA under project identifier PRJEB6344 (exome capture), BAC raw data under identifier PRJEB11284, assembled BAC sequences as accessions LO018452 to LO018472, and WGS raw data of BW457 are available under project PRJEB3038. Gene reference sequences from Sanger sequencing are available at EMBL-ENA (*HvLax-a*, LN897709; *HvCul4*, LN897710).

Supplemental Data

The following supplemental materials are available.

Supplemental Figure S1. Rachis internode length in *lax-a* mutant and wild-type plants.

Supplemental Figure S2. Genetic mapping.

Supplemental Figure S3. Exome-capture SNP plots.

Supplemental Figure S4. Sequence analysis of FPC_2862 containing the *HvLax-a* candidate gene.

Supplemental Figure S5. Independent *lax-a* mutant alleles and allelism test.

Supplemental Figure S6. BOP/ANK gene family of Arabidopsis and barley.

Supplemental Figure S7. Phenotypes of mutants obtained by TILLING of *HvCul4*.

Supplemental Figure S8. Phylogenetic analysis of *BOP-like* genes in the plant kingdom.

Supplemental Figure S9. Expression of barley *BOP-like* genes during barley development.

Supplemental Table S1. Statistics of target enrichment sequencing.

Supplemental Table S2. Filter for cosegregating targets with expected SNP frequency within captured pools.

Supplemental Table S3. Exome-capture targets with SNPs that cosegregate with the *HvLax-a* phenotype.

Supplemental Table S4. Filtered candidate targets of read coverage analysis within captured pools.

Supplemental Table S5. Targets with low coverage in captured pools with the mutant phenotype.

Supplemental Table S6. Sequenced BACs.

Supplemental Table S7. Genes on sequenced BACs of FPC_2862.

Supplemental Table S8. Identified TILLING mutants within *HvLax-a*.

Supplemental Table S9. Identified TILLING mutants for *HvCul4*.

Supplemental Table S10. Information for the plant material used to identify sequence haplotypes of *HvLax-a* and *HvCul4*.

Supplemental Table S11. Oligonucleotides of *HvLax-a*.

Supplemental Table S12. SNP marker used for the F1 test.

Supplemental Table S13. Marker information of genetic mapping.

Supplemental Table S14. SNaPshot genotyping assays.

Supplemental Table S15. Oligonucleotides of *HvCul4*.

ACKNOWLEDGMENTS

LITERATURE CITED

Altschul SF, Gish W, Miller W, Myers EW, Lipman DJ (1990) Basic local alignment search tool. J Mol Biol **215:** 403–410

Andrés F, Romera-Branchat M, Martínez-Gallegos R, Patel V, Schneeberger K, Jang S, Altmüller J, Nürnberg P, Coupland G (2015) Floral induction in Arabidopsis by *FLOWERING LOCUS T* requires direct repression of *BLADE-ON-PETIOLE* genes by the homeodomain protein PENNYWISE. Plant Physiol **169:** 2187–2199

Ariyadasa R, Mascher M, Nussbaumer T, Schulte D, Frenkel Z, Poursarebani N, Zhou R, Steuernagel B, Gundlach H, Taudien S, et al (2014) A sequence-ready physical map of barley anchored genetically by two million single-nucleotide polymorphisms. Plant Physiol **164:** 412–423

Bandelt HJ, Forster P, Röhl A (1999) Median-joining networks for inferring intraspecific phylogenies. Mol Biol Evol **16:** 37–48

Begun DJ, Aquadro CF (1992) Levels of naturally occurring DNA polymorphism correlate with recombination rates in D. melanogaster. Nature **356:** 519–520

Beier S, Himmelbach A, Schmutzer T, Felder M, Taudien S, Mayer K, Platzer M, Stein N, Scholz U, Mascher M (2015) Multiplex sequencing of bacterial artificial chromosomes for assembling complex plant genomes. Plant Biotechnol J in press doi:10.1111/pbi.12511

Canet JV, Dobón A, Fajmonová J, Tornero P (2012) The *BLADE-ON-PETIOLE* genes of Arabidopsis are essential for resistance induced by methyl jasmonate. BMC Plant Biol **12:** 199

Close TJ, Bhat PR, Lonardi S, Wu Y, Rostoks N, Ramsay L, Druka A, Stein N, Svensson JT, Wanamaker S, et al (2009) Development and implementation of high-throughput SNP genotyping in barley. BMC Genomics **10:** 582

Doyle JJ, Doyle JL (1990) Isolation of plant DNA from fresh tissue. Focus **12:** 13–15

Druka A, Franckowiak J, Lundqvist U, Bonar N, Alexander J, Houston K, Radovic S, Shahinnia F, Vendramin V, Morgante M, et al (2011) Genetic dissection of barley morphology and development. Plant Physiol **155:** 617–627

Edgar RC (2004a) MUSCLE: a multiple sequence alignment method with reduced time and space complexity. BMC Bioinformatics **5:** 113

Edgar RC (2004b) MUSCLE: multiple sequence alignment with high accuracy and high throughput. Nucleic Acids Res **32:** 1792–1797

Ewing B, Green P (1998) Base-calling of automated sequencer traces using phred. II. Error probabilities. Genome Res **8:** 186–194

Ewing B, Hillier L, Wendl MC, Green P (1998) Base-calling of automated sequencer traces using phred. I. Accuracy assessment. Genome Res **8:** 175–185

Forster BP, Franckowiak JD, Lundqvist U, Lyon J, Pitkethly I, Thomas WT (2007) The barley phytomer. Ann Bot (Lond) **100:** 725–733

Franckowiak JD, Lundqvist U (2010) Descriptions of barley genetic stocks for 2010. Genetics Newsletter **40:** 45–177

Gottwald S, Bauer P, Komatsuda T, Lundqvist U, Stein N (2009) TILLING in the two-rowed barley cultivar 'Barke' reveals preferred sites of functional diversity in the gene *HvHox1*. BMC Res Notes **2:** 258

Ha CM, Jun JH, Nam HG, Fletcher JC (2004) *BLADE-ON-PETIOLE1* encodes a BTB/POZ domain protein required for leaf morphogenesis in Arabidopsis thaliana. Plant Cell Physiol **45:** 1361–1370

Ha CM, Jun JH, Nam HG, Fletcher JC (2007) *BLADE-ON-PETIOLE1* and *2* control *Arabidopsis* lateral organ fate through regulation of LOB domain and adaxial-abaxial polarity genes. Plant Cell **19:** 1809–1825

Hall BG (2013) Building phylogenetic trees from molecular data with MEGA. Mol Biol Evol **30:** 1229–1235

Hamant O, Pautot V (2010) Plant development: a TALE story. C R Biol **333:** 371–381

Haseneyer G, Stracke S, Paul C, Einfeldt C, Broda A, Piepho HP, Graner A, Geiger HH (2010) Population structure and phenotypic variation of a spring barley world collection set up for association studies. Plant Breed **129:** 271–279

Hay A, Tsiantis M (2010) *KNOX* genes: versatile regulators of plant development and diversity. Development **137:** 3153–3165

Hepworth SR, Zhang Y, McKim S, Li X, Haughn GW (2005) *BLADE-ON-PETIOLE*-dependent signaling controls leaf and floral patterning in *Arabidopsis*. Plant Cell **17:** 1434–1448

Himmelbach A, Knauft M, Stein N (2014) Plant sequence capture optimised for Illumina sequencing. Bio Protoc **4:** 1–23

Horigome A, Nagasawa N, Ikeda K, Ito M, Itoh J, Nagato Y (2009) Rice *open beak* is a negative regulator of *class 1 knox* genes and a positive regulator of class B floral homeotic gene. Plant J **58:** 724–736

Houston K, Druka A, Bonar N, Macaulay M, Lundqvist U, Franckowiak J, Morgante M, Stein N, Waugh R (2012) Analysis of the barley bract suppression gene *Trd1*. Theor Appl Genet **125:** 33–45

Houston K, McKim SM, Comadran J, Bonar N, Druka I, Uzrek N, Cirillo E, Guzy-Wrobelska J, Collins NC, Halpin C, et al (2013) Variation in the interaction between alleles of *HvAPETALA2* and microRNA172 determines the density of grains on the barley inflorescence. Proc Natl Acad Sci USA **110:** 16675–16680

Jun JH, Ha CM, Fletcher JC (2010) *BLADE-ON-PETIOLE1* coordinates organ determinacy and axial polarity in *Arabidopsis* by directly activating *ASYMMETRIC LEAVES2*. Plant Cell **22:** 62–76

Karim MR, Hirota A, Kwiatkowska D, Tasaka M, Aida M (2009) A role for *Arabidopsis* PUCHI in floral meristem identity and bract suppression. Plant Cell **21:** 1360–1372

Kellogg EA (2001) Evolutionary history of the grasses. Plant Physiol 125: 1198–1205

Khan M, Ragni L, Tabb P, Salasin BC, Chatfield S, Datla R, Lock J, Kuai X, Despres C, Proveniers M, Proveniers M, Yongguo C, Xiang D, Morin H, Rulliere JP, Citerne S, Hepworth SR, Pautot V (2015) Repression of Lateral Organ Boundary Genes by PENNYWISE and POUND-FOOLISH Is Essential for Meristem Maintenance and Flowering in Arabidopsis. Plant Physiol 169: 2166–2186

Khan M, Tabb P, Hepworth SR (2012b) *BLADE-ON-PETIOLE1* and *2* regulate Arabidopsis inflorescence architecture in conjunction with homeobox genes KNAT6 and ATH1. Plant Signal Behav 7: 788–792

Khan M, Xu H, Hepworth SR (2014) *BLADE-ON-PETIOLE* genes: setting boundaries in development and defense. Plant Sci 215-216: 157–171

Khan M, Xu M, Murmu J, Tabb P, Liu Y, Storey K, McKim SM, Douglas CJ, Hepworth SR (2012a) Antagonistic interaction of *BLADE-ON-PETIOLE1* and *2* with *BREVIPEDICELLUS* and *PENNYWISE* regulates Arabidopsis inflorescence architecture. Plant Physiol 158: 946–960

Kircher M, Sawyer S, Meyer M (2012) Double indexing overcomes inaccuracies in multiplex sequencing on the Illumina platform. Nucleic Acids Res 40: e3

Komatsuda T, Pourkheirandish M, He C, Azhaguvel P, Kanamori H, Perovic D, Stein N, Graner A, Wicker T, Tagiri A, et al (2007) Six-rowed barley originated from a mutation in a homeodomain-leucine zipper I-class homeobox gene. Proc Natl Acad Sci USA 104: 1424–1429

Konieczny A, Ausubel FM (1993) A procedure for mapping Arabidopsis mutations using co-dominant ecotype-specific PCR-based markers. Plant J 4: 403–410

Koppolu R, Anwar N, Sakuma S, Tagiri A, Lundqvist U, Pourkheirandish M, Rutten T, Seiler C, Himmelbach A, Ariyadasa R, et al (2013) *Six-rowed spike4* (*Vrs4*) controls spikelet determinacy and row-type in barley. Proc Natl Acad Sci USA 110: 13198–13203

Kyozuka J, Shimamoto K (2002) Ectopic expression of *OsMADS3*, a rice ortholog of *AGAMOUS*, caused a homeotic transformation of lodicules to stamens in transgenic rice plants. Plant Cell Physiol 43: 130–135

Larsson HEB (1985) Morphological analysis of laxatum barley mutants. Hereditas 103: 239–253

Laurie DA, Pratchett N, Allen RL, Hantke SS (1996) RFLP mapping of the barley homeotic mutant *lax-a*. Theor Appl Genet 93: 81–85

Li H (2011) A statistical framework for SNP calling, mutation discovery, association mapping and population genetical parameter estimation from sequencing data. Bioinformatics 27: 2987–2993

Li H, Durbin R (2009) Fast and accurate short read alignment with Burrows-Wheeler transform. Bioinformatics 25: 1754–1760

Li X, Zhang Y (2002) Reverse genetics by fast neutron mutagenesis in higher plants. Funct Integr Genomics 2: 254–258

Librado P, Rozas J (2009) DnaSP v5: a software for comprehensive analysis of DNA polymorphism data. Bioinformatics 25: 1451–1452

Lundqvist U (2009) Eighty years of Scandinavian barley mutation genetics and breeding. *In* Induced Plant Mutations in the Genomics Era. Food and Agriculture Organization of the United Nations, Rome, pp 39–43

Mascher M, Jost M, Kuon JE, Himmelbach A, Aßfalg A, Beier S, Scholz U, Graner A, Stein N (2014) Mapping-by-sequencing accelerates forward genetics in barley. Genome Biol 15: R78

Mascher M, Richmond TA, Gerhardt DJ, Himmelbach A, Clissold L, Sampath D, Ayling S, Steuernagel B, Pfeifer M, D'Ascenzo M, et al (2013a) Barley whole exome capture: a tool for genomic research in the genus Hordeum and beyond. Plant J 76: 494–505

Mascher M, Wu S, Amand PS, Stein N, Poland J (2013b) Application of genotyping-by-sequencing on semiconductor sequencing platforms: a comparison of genetic and reference-based marker ordering in barley. PLoS ONE 8: e76925

Mayer KF, Martis M, Hedley PE, Simková H, Liu H, Morris JA, Steuernagel B, Taudien S, Roessner S, Gundlach H, et al (2011) Unlocking the barley genome by chromosomal and comparative genomics. Plant Cell 23: 1249–1263

Mayer KF, Waugh R, Brown JW, Schulman A, Langridge P, Platzer M, Fincher GB, Muehlbauer GJ, Sato K, Close TJ, et al (2012) A physical, genetic and functional sequence assembly of the barley genome. Nature 491: 711–716

McKim SM, Stenvik GE, Butenko MA, Kristiansen W, Cho SK, Hepworth SR, Aalen RB, Haughn GW (2008) The *BLADE-ON-PETIOLE* genes are essential for abscission zone formation in Arabidopsis. Development 135: 1537–1546

Michelmore RW, Paran I, Kesseli RV (1991) Identification of markers linked to disease-resistance genes by bulked segregant analysis: a rapid method to detect markers in specific genomic regions by using segregating populations. Proc Natl Acad Sci USA 88: 9828–9832

Müller KJ, Romano N, Gerstner O, Garcia-Maroto F, Pozzi C, Salamini F, Rohde W (1995) The barley *Hooded* mutation caused by a duplication in a homeobox gene intron. Nature 374: 727–730

Nair SK, Wang N, Turuspekov Y, Pourkheirandish M, Sinsuwongwat S, Chen G, Sameri M, Tagiri A, Honda I, Watanabe Y, et al (2010) Cleistogamous flowering in barley arises from the suppression of microRNA-guided *HvAP2* mRNA cleavage. Proc Natl Acad Sci USA 107: 490–495

Norberg M, Holmlund M, Nilsson O (2005) The *BLADE ON PETIOLE* genes act redundantly to control the growth and development of lateral organs. Development 132: 2203–2213

Pasam RK, Sharma R, Malosetti M, van Eeuwijk FA, Haseneyer G, Kilian B, Graner A (2012) Genome-wide association studies for agronomical traits in a world wide spring barley collection. BMC Plant Biol 12: 16

Pourkheirandish M, Hensel G, Kilian B, Senthil N, Chen G, Sameri M, Azhaguvel P, Sakuma S, Dhanagond S, Sharma R, et al (2015) Evolution of the grain dispersal system in barley. Cell 162: 527–539

Poursarebani N, Seidensticker T, Koppolu R, Trautewig C, Gawroński P, Bini F, Govind G, Rutten T, Sakuma S, Tagiri A, et al (2015) The genetic basis of composite spike form in barley and 'Miracle-Wheat'. Genetics 201: 155–165

Quinlan AR, Hall IM (2010) BEDTools: a flexible suite of utilities for comparing genomic features. Bioinformatics 26: 841–842

Ramsay L, Comadran J, Druka A, Marshall DF, Thomas WT, Macaulay M, MacKenzie K, Simpson C, Fuller J, Bonar N, et al (2011) *INTERMEDIUM-C*, a modifier of lateral spikelet fertility in barley, is an ortholog of the maize domestication gene *TEOSINTE BRANCHED 1*. Nat Genet 43: 169–172

Schneeberger K, Weigel D (2011) Fast-forward genetics enabled by new sequencing technologies. Trends Plant Sci 16: 282–288

Schulte D, Ariyadasa R, Shi B, Fleury D, Saski C, Atkins M, deJong P, Wu CC, Graner A, Langridge P, et al (2011) BAC library resources for map-based cloning and physical map construction in barley (Hordeum vulgare L.). BMC Genomics 12: 247

Stein N, Graner A (2005) Map-based gene isolation in cereal genomes. *In* PK Gupta, RK Varshney, eds, Cereal Genomics. Kluwer Academic Publishers, Dordrecht, The Netherlands, pp 331–360

Stein N, Herren G, Keller B (2001) A new DNA extraction method for high-throughput marker analysis in a large-genome species such as Triticum aestivum. Plant Breed 120: 354–356

Tajima F (1989) Statistical method for testing the neutral mutation hypothesis by DNA polymorphism. Genetics 123: 585–595

Taketa S, Amano S, Tsujino Y, Sato T, Saisho D, Kakeda K, Nomura M, Suzuki T, Matsumoto T, Sato K, et al (2008) Barley grain with adhering hulls is controlled by an *ERF* family transcription factor gene regulating a lipid biosynthesis pathway. Proc Natl Acad Sci USA 105: 4062–4067

Tamura K, Stecher G, Peterson D, Filipski A, Kumar S (2013) MEGA6: Molecular Evolutionary Genetics Analysis version 6.0. Mol Biol Evol 30: 2725–2729

Tanaka W, Toriba T, Ohmori Y, Yoshida A, Kawai A, Mayama-Tsuchida T, Ichikawa H, Mitsuda N, Ohme-Takagi M, Hirano HY (2012) The *YABBY* gene *TONGARI-BOUSHI1* is involved in lateral organ development and maintenance of meristem organization in the rice spikelet. Plant Cell 24: 80–95

Tavakol E, Okagaki R, Verderio G, Shariati J V, Hussien A, Bilgic H, Scanlon MJ, Todt NR, Close TJ, Druka A, et al (2015) The barley *Uniculme4* gene encodes a BLADE-ON-PETIOLE-like protein that controls tillering and leaf patterning. Plant Physiol 168: 164–174

Whipple CJ, Hall DH, DeBlasio S, Taguchi-Shiobara F, Schmidt RJ, Jackson DP (2010) A conserved mechanism of bract suppression in the grass family. Plant Cell 22: 565–578

Xiao H, Tang J, Li Y, Wang W, Li X, Jin L, Xie R, Luo H, Zhao X, Meng Z, et al (2009) *STAMENLESS 1*, encoding a single C2H2 zinc finger protein, regulates floral organ identity in rice. Plant J 59: 789–801

Xu M, Hu T, McKim SM, Murmu J, Haughn GW, Hepworth SR (2010) Arabidopsis *BLADE-ON-PETIOLE1* and *2* promote floral meristem fate and determinacy in a previously undefined pathway targeting *APETALA1* and *AGAMOUS-LIKE24*. Plant J 63: 974–989

Yuo T, Yamashita Y, Kanamori H, Matsumoto T, Lundqvist U, Sato K, Ichii M, Jobling SA, Taketa S (2012) A *SHORT INTERNODES* (*SHI*) family transcription factor gene regulates awn elongation and pistil morphology in barley. J Exp Bot 63: 5223–5232